MICROBUBBLE SKIN FRICTION REDUCTION ON AN AXISYMMETRIC BODY

S. Deutsch and J. Castano

Technical Memorandum
File No. TM 85-139
2 August 1985
Contract N00024-79-C-6043

Copy No. 1

The Pennsylvania State University
Intercollege Research Programs and Facilities
APPLIED RESEARCH LABORATORY
Post Office Box 30
State College, PA 16804

Approved for Public Release

NAVY DEPARTMENT

NAVAL SEA SYSTEMS COMMAND

SECURITY CLASSIFICATION OF THIS PAGE (When Data Entered)

REPORT DOCUMENTATION PAGE

READ INSTRUCTIONS BEFORE COMPLETING FORM

1. REPORT NUMBER: TM 85-139	2. GOVT ACCESSION NO.
3. RECIPIENT'S CATALOG NUMBER	
4. TITLE (and Subtitle): MICROBUBBLE SKIN FRICTION REDUCTION ON AN AXISYMMETRIC BODY	5. TYPE OF REPORT & PERIOD COVERED: Technical Memorandum
	6. PERFORMING ORG. REPORT NUMBER
7. AUTHOR(s): S. Deutsch and J. Castano	8. CONTRACT OR GRANT NUMBER(s): N00024-79-C-6043
9. PERFORMING ORGANIZATION NAME AND ADDRESS: Applied Research Laboratory, The Pennsylvania State University, State College PA 16804	10. PROGRAM ELEMENT, PROJECT, TASK AREA & WORK UNIT NUMBERS
11. CONTROLLING OFFICE NAME AND ADDRESS: Naval Sea Systems Command, Code NSEA 63R-31, Department of the Navy, Washington DC 20362	12. REPORT DATE: 2 August 1985
	13. NUMBER OF PAGES: 26
14. MONITORING AGENCY NAME & ADDRESS (if different from Controlling Office)	15. SECURITY CLASS. (of this report): Unclassified
	15a. DECLASSIFICATION/DOWNGRADING SCHEDULE

16. DISTRIBUTION STATEMENT (of this Report)

Approved for public release. Distribution unlimited.
Per NAVSEA - 12 September 1985.

17. DISTRIBUTION STATEMENT (of the abstract entered in Block 20, if different from Report)

18. SUPPLEMENTARY NOTES

19. KEY WORDS (Continue on reverse side if necessary and identify by block number)

20. ABSTRACT (Continue on reverse side if necessary and identify by block number)

A reduction in skin friction drag is shown when gas is introduced into the liquid turbulent boundary layer of a submerged axisymmetric body. The 89 mm diameter, 632 mm long body has an cylindrical balance 273 mm long. Free stream speeds in the 305 mm diameter tunnel are as high as 17 m/sec, giving length Reynolds numbers of up to 10 million. In general, skin friction reduction is shown to increase with increasing free stream speed. At high speeds, helium injection is shown to be more effective at reducing skin friction

DD FORM 1 JAN 73 1473 EDITION OF 1 NOV 65 IS OBSOLETE

SECURITY CLASSIFICATION OF THIS PAGE (When Data Entered)

than is air injection. Maximum skin friction reduction is near 80% -- a value in good agreement, with the maximum value observed in the flat plate work of Madavan, Deutsch and Merkle (MDM). Maximum skin friction reduction is found at 17 m/sec for the axisymmetric case, however, as opposed to 5 m/sec for flat plate work.

From: S. Deutsch and J. Castano

Subject: Microbubble Skin Friction Reduction on an Axisymmetric Body

Abstract: A reduction in skin friction drag is shown when gas is introduced into the liquid turbulent boundary layer of a submerged axisymmetric body. The 89 mm diameter, 632 mm long body has an cylindrical balance 273 mm long. Free stream speeds in the 305 mm diameter tunnel are as high as 17 m/sec, giving length Reynolds numbers of up to 10 million. In general, skin friction reduction is shown to increase with increasing free stream speed. At high speeds, helium injection is shown to be more effective at reducing skin friction than is air injection. Maximum skin friction reduction is near 80% --a value in good agreement with the maximum value observed in the flat plate work of Madavan, Deutsch and Merkle (MDM). Maximum skin friction reduction is found at 17 m/sec for the axisymmetric case, however, as opposed to 5 m/sec for flat plate work.

Introduction

The injection of a gas (to form microbubbles) into a liquid turbulent boundary layer has been shown, in several studies [1-8], to reduce drag. For the most part, these studies have looked at the skin friction reduction obtainable in a flat plate geometry [1-7]. The drag reduction mechanism is not very well understood; only two rudimentary analytical/computational studies [9,10] have been attempted. While the key to a fundamental understanding of the phenomenon would appear to lie in an understanding of bubble dynamics in a boundary layer flow, it seems plausible from the computational work [9], when taken in concert with some bubble concentration profile measurements [4-6], that the bubbles provide a mechanism for increasing the kinematic viscosity near the buffer region, thereby destroying some of the turbulent production. A similar mechanism has been postulated for the polymer drag reduction phenomenon [11].

In the current study, the series of microbubble skin friction reduction experiments is extended to a more practical, axisymmetric geometry. The scope of the study is very much like that undertaken by MDM [1]. Before describing the current set of experiments and their results, however, we present a summary of previous work done on microbubble drag reduction. A more detailed review has been given by Merkle and Deutsch [12].

Measurements of drag reduction by microbubbles was first reported by McCormick and Bhattacharyya in 1973 [8]. This was the only reported study in which total, as opposed to skin friction drag, was measured. A 914.4 mm long, 127 mm (maximum) diameter axisymmetric body was used in the experiment. A 0.15 mm diameter copper wire was wound around the hull in order to generate microbubbles through electrolysis. The number of coils, the amount of surface area over which they extended and the initial coil locations were all varied. The model was run in a tow tank at speeds between 0.32 and 2.6 m/sec. Maximum length Reynolds numbers varied from 0.3 to 2.4 million. The undisturbed boundary layer characteristics were not measured. The rate of hydrogen mass production was estimated using Faraday's law; the volumetric flow rates were between 1.35×10^{-4} and 4.1×10^{-4} m^3/sec.

McCormick and Bhattacharyya found higher drag reduction when the coils were extended over a larger surface area (except at the higher model speeds at which a bubble induced premature separation probably occurred). Inconclusive results were found when the coils were only extended over a small (19%) area immediately behind the boundary layer trip. It seems likely that for this case the bubbles hastened transition -- causing some increased drag. The tests made with variable gas flow rates showed that drag reduction increased with gas flow rate; a maximum reduction of near 30% in total drag was observed at a model speed of 1.28 m/sec and maximum gas flow rate. In general, the largest reductions were observed at the lower model velocities, perhaps because of insufficient hydrogen gas generation for the higher speeds (i.e., a small ratio of gas to water volume flow rate).

Several Soviet studies followed the McCormick and Bhattacharrya work. Perhaps the most comprehensive Soviet investigation on microbubble drag reduction was carried out by Migirenko and Evseev [4] in 1974. A 955 mm long flat plate, 224 mm wide and 40 mm thick, was suspended in the center of a (roughly 244 × 150 mm) 1.5 m long rectangular test section. The porous section, which began at 79.2 mm and ended at 401 mm from the leading edge, was made up of 0.8 mm thick, machine-etched aluminum plates compressed together and mounted flush to the top surface of the flat plate. Pore size was estimated by empirical relationships based on the bubble separation diameter (defined as the diameter of the bubbles immediately after separation from the porous material) which was measured from photographs of bubbles in quiescent water. The permeable plate was estimated to have a pore size of between 0.5 and 3.5 microns and a porosity of 1%.

The local skin friction was measured by a floating wall sensor (at an unspecified distance) downstream of the porous section. The sketch presented suggests that the sensor is roughly 450 mm from the leading edge of the plate. Note that the sensor is on the top surface of the plate, so that buoyancy would tend to remove bubbles from the boundary layer. The bubble concentration in the boundary layer was measured by a conductivity probe; pressure fluctuations were also measured (but in an unspecified manner).

Maximum gas flow rates used were between 0.8×10^{-3} and 1.85×10^{-3} m^3/sec. Reductions in skin friction drag were found for the four mean flow velocities (4.4, 6.5, 8.7 and 10.9 m/sec) tested. At the higher velocities the skin friction reduction increased monotonically with gas flow rate; the drag was reduced to nearly 10% of its no gas value at 10.9 m/sec and maximum gas flow rate. The drag response at the lower (4.4 and 6.5 m/sec) velocities was quite different; an initial rise in drag was followed by a steady drop to a maximally reduced drag, after which the drag began to rise again with gas flow rate. In general, reductions in drag increased with mean velocity for a given gas flow rate.

The conductivity probe measurements showed that for a given gas flow rate the location of the maximum bubble concentration approached the surface as the mean flow velocity increased. At the highest tunnel velocity and the maximum gas flow rate, a peak bubble concentration of 0.75 was found at a distance from the surface at which Y/δ is 0.1.

Other Soviet experiments were made by Dubnishchev et al. [5] (as reported in Migirenko and Evseev [4]) and by Bogdevich and Maligua [6]. Bogdevich and Evseev [7] reviewed several of the Soviet experiments.

The most recent series of experiments in microbubble drag reduction were performed by Madavan, Deutsch and Merkle [1-3] in a 508 × 114 mm rectangular test section 762 mm long. The flat plate configuration employed was mounted flush to a tunnel wall in a 279 × 533 mm slot intended for a window. A 102 mm wide by 178 mm long porous section was placed in front of a force balance 102

x 254 mm long. For the initial tests, the porous section was constructed from a sintered stainless steel filter material with a nominal pore size of 5 microns. The orientation of the plate with respect to gravity was varied by rotating the test section. Tests were made with the plate above, below and alongside the microbubble filled turbulent boundary layer.

Mean velocity and turbulent intensity profiles were measured at three streamwise locations in the undisturbed boundary layer. The profiles appeared to be fully developed at speeds above 5 m/sec. Length Reynolds numbers, based on a fictitious boundary layer origin, deduced from the velocity profiles, were between 2.2 and 10.6 million. Static pressure measurements showed the pressure gradient to be nominally zero over the length of the test plate.

Integrated skin friction on the floating element force balance was measured at free-stream speeds of 4.2 to 17.4 m/sec. The results show skin friction reductions ranging from 50 to 80% (depending on plate orientation) at a maximum air flow rate near 5×10^{-3} m^3/sec. The largest reductions occurred for the plate on top case where buoyancy tended to keep the bubbles in the boundary layer. In contrast to the results of Migirenko and Evseev [4] maximum drag reduction was found at the lowest speed tested. This would appear to indicate that buoyancy was not a major factor in the MDM tests, but rather that the drag reduction was limited by the availability of gas at the higher tunnel speeds*. MDM [1] also performed some limited experiments with helium. Helium injection was found to give the same reduction as air injection, indicating that the density of the gas was not a variable.

In the initial MDM experiments [1], the local skin friction was measured by a surface mounted hot film probe located 51 mm from the trailing edge of the porous material. For the plate on the bottom orientation, local reductions of nearly 90% were observed. MDM reported that oscilloscope traces of the hot film probe output signal showed no sign of bubble impingement (as opposed to a hot film probe in the boundary layer, say). This confirmed the concentration measurements made by Bogdevich and Maliuga [6] which indicated that the bubbles were not present in the region (sublayer) closest to the wall. This apparent lack of bubbles in the very near wall region is important, if one is to believe that a major mechanism for bubble drag reduction is the selective increase of kinematic viscosity (in the buffer region).

A second series of experiments, employing an array of hot film probes on the balance was also conducted by MDM [2]. Using this array they were able to show that substantial drag reduction persisted for as much as 60 to 70 boundary layer thicknesses downstream of the injection section. The loss of some of the turbulent production scales was confirmed through

*Note that the work of MDM [1-3] and Migirenko and Evseev [4] complement rather than contradict each other. Some unpublished work by MDM indicates that the drag reduction decreases as the free stream speed is reduced below about 4 m/sec and buoyant effects become large.

spectral measurements; the similarity between the shear stress spectrum for the microbubble boundary layer and the polymer boundary layer [13] was quite striking.

In the current experiment, skin friction drag measurements are extended to an axisymmetric body. To facilitate comparison between the current study and the work of MDM [1], some boundary layer parameters are presented for each in Table 1. These are the only two studies for which details of the undisturbed boundary layer are available.

Facilities and Procedures

The current experiment was run in the 305 mm diameter tunnel at the Applied Research Laboratory of The Pennsylvania State University. This tunnel, but with the rectangular section in place, was previously described by MDM [1]. Tunnel velocity, pressure and gas injection flow rates were controlled manually. The tunnel has a bypass mechanism to purge the water of gas accumulation; in general, this allowed for long periods of continuous gas injection without serious fluctuations in the tunnel speed and pressure. Data acquisition and reduction were accomplished through an on-line VAX 11/780 computer system.

Figure 1 shows the 89 mm diameter axisymmetric model. The overall length of the model is 632 mm. An isolated cylindrical section with stiff tension/compression members serves as a force balance to measure the skin friction; the balance is 273 mm long with gaps of 0.127 and 0.254 mm located at axial distances of 196 and 469 mm from the nose respectively. The gaps were carefully aligned to minimize potential pressure effects. Maximum balance displacement was estimated to be no more than 50 microns. A 6.35 mm long and 5.17 mm thick, cylindrical, sintered porous plastic section, with a nominal pore size of 5 microns, was used to inject the gas at a distance of 146.5 mm from the nose. Moveable partitions, inside the model, were set to visually ensure symmetric gas injection over the model. A steel wire, 0.35 mm in diameter, was placed 46 mm from the leading edge in an effort to trip the boundary layer and ensure a fully-developed turbulent boundary layer over the measuring section. A 200 mm long sting mount held the model in the center of the test section; two 127 mm long streamlined struts inclined at 45 degrees from the sting were attached to the lower tunnel wall immediately behind the model. Identical dummy struts were placed symmetrically opposite the support struts to preserve flow symmetry.

The balance employed a strain-gauged tension compression member to infer the integrated skin friction on the surface. The balance was dry calibrated in place in the test section using a radially centered pulley and incremental weights. The balance showed excellent linearity. Several of the calibrations were made with air injection and showed that injection had no effect on the measured drag. Throughout the test program the response of the balance was checked against tunnel speed for consistency; no measurable drift was noted.

Reference drag tests provided skin friction drag as a function of the mean flow speed. Small random fluctuations in velocity (during injection*) were accounted for by normalizing the drag measured by the balance during gas injection with the reference drag calculated at the actual velocity (determined from a second order least squares curve fit of the calibration data). The velocity corrected tests were then arranged by the test "target" velocity (6.1, 10.7 or 16.8 m/sec) and sorted into bins according to gas flow rate. The number of data points in each bin was equal to the number of runs made at each target velocity with a given gas. A student T-test was used to calculate 95% confidence levels for the data in each bin. This provided one curve of normalized drag reduction against gas flow rate for each gas at each of the target velocities.

The gas volume flow rate, the free stream velocity and the type of gas (air or helium) were systematically varied to determine the influence each had on the skin friction. Gas injection flow rates were measured with an rotameter. The rotatmeter was calibrated to measure air flow rates at standard atmospheric pressure and temperature. Gas flow rates were corrected for the actual injection pressure and for the density of the injected gas. Gas temperature was not measured during injection, but subsequent bench tests indicated that both gases were injected at near room temperature for the range of pressures and flow rates employed.

An LDV was used to measure the velocity profiles at three locations (4.7, 134.9 and 265.1 mm from the upstream gap) on the balance to determine the characteristics of the undisturbed boundary layer. The LDV was composed of a spectra-physics 8-Watt argon-ion laser and power supply, and TSI optics consisting of a 3.75X beam expander, a 460 mm transmitting lens, and a model 1980 counter processor. A small amount of 1.5 micron silicon-carbide particles was added to the tunnel as seed. Data reduction was through the VAX 11/780 computer. An aluminum collar with a scribed line 7.93 mm above the surface of the balance was used to find a consistent reference point for the LDV sample volume, in this way providing a known initial position in the boundary layer. Experience with these templates indicates a repeatability in the initial location of some 50 microns. The single component, dual beam system was operated in the backscatter mode. The turbulence intensity dictated the number of samples that was taken at each point in the boundary layer; 200 points for turbulence intensities below 5%, 500 samples for turbulence intensities below 10% and 1,000 samples for turbulence intensities above 10%. The number of samples was chosen, in each case, to insure reasonable repeatability of the mean velocity and the turbulence intensity.

The static pressure distribution along the test section wall was measured using a bank of individual pressure transducers. The pressure was measured at six axial locations, 104 mm apart along the wall, with the first tap positioned 109.5 mm downstream of the nose. At each of the axial locations, a pressure reading was taken from each of the four quadrants of the circular test section in order to check for axial-symmetry. The pressure tap in each

*These velocity fluctuations arise because of the large amount of air the tunnel impeller encounters. Such free stream gas contamination has been shown to have no effect on the drag characteristics.

quadrant was lined up circumferentially with the support and dummy support struts. Each survey of the 24 pressure taps lasted approximately four seconds. Test runs made at constant tunnel speed indicated that this was sufficiently fast so that tunnel velocity variations did not contaminate the results. Surveys were taken at 20 to 30 air injection rates (to 3.6×10^{-3} m^3/sec) to test for possible pressure variations or flow asymmetry with injection. It should be noted that the free stream velocity at the model was calculated from measurements made by differencing the settling section pressure against the static pressure at the second tap location in the test section (213.5 mm from the nose). Approach velocities were then some 10% lower.

Results

The skin friction coefficient (based on the surface area of the balance) is shown as a function of Reynolds number (based on the maximum model diameter) in Fig. 2. The tests presented span the period of the experimentaton and are characteristic of data taken for both increasing and decreasing tunnel speed. With the exception of the data taken at the lowest speeds, at which deviations between runs are as high as 10%, repeatability is excellent. The low speed deviations are characteristic, and represent a balance sensitivity problem at very low force values. This problem re-emerges in the large error bands associated with the skin friction reduction data taken at a free stream speed of 4.6 m/sec.

LDV surveys of the boundary layer, at 4.7, 134.9 and 265.1 mm downstream of the upstream gap, were taken at free stream speeds of 5.0, 11.1 and 17.2 m/sec. Data reduction was through an existing code [14], which for these measurements may be considered to be an automated "Clauser plot" technique. In general, measurements could be made no closer than a Y_+ of 100, which corresponded to a U/U_∞ of about 0.6. A sufficient number of points were obtained in the logarithmic region for the shear velocity to be estimated. Comparisons between the shear stress on the balance (taken as the average of the three measured values at each speed) as obtained from the fit of the LDV data to the law of the wall, against the shear stress obtained from the balance measurements agreed to within 10%. For velocities above 5 m/sec the profiles appear to be fully developed. Important boundary layer parameters are shown, along with a comparison with the MDM [1] data, in Table 1. Note that although the outer scales were as much as twice as large in the MDM [1] experiments than in the current study, the inner scale, u^*, compares to within about 15%. Shape factors are almost identical.

As noted earlier, the symmetry of the flow during air injection was checked by comparing the wall static pressure distribution taken along the four quadrants of the tunnel test section, at six axial locations. A typical normalized velocity distribution is given as a function of the pressure tap axial location in Fig. 3. For convenience in interpreting the plot, the location of the balance section is included in the figure. Note that the flow exhibits excellent axial-symmetry both with and without gas injection. In all cases the velocity is reasonably constant across the balance section, indicating the presence of a zero pressure gradient flow --

a result which does not change with gas injection. The strong decrease in velocity at the last pressure tap is caused by the increased flow area as the tail of the body is approached.

The skin friction drag reduction data are presented for free stream velocities of 4.6, 7.6, 10.7 and 16.8 m/sec in Figs. 4 through 6. The boundary layer at 4.6 m/sec is probably not fully-developed. Mean drag reduction data are presented as the ratio of skin friction coefficient to the no gas injection skin friction coefficient, against the gas volumetric flow rate. The range of gas volumetric flow rates employed in the MDM work is shown, for convenience, on the figures. Also shown in the figures are 95% confidence levels as determined by a student T-test.

The data taken at 4.6 m/sec shows that the drag, at the lowest gas flow rates, initially increases with the gas injection. This suggests that the injection may be hastening the transition of an under-developed boundary layer at this low speed. A maximum drag reduction, of 20% for air and 15% for helium, occurs at gas flow rates between 1.5 and 2.5 $\times 10^{-3}$ m^3/sec. Increasing the gas flow rate further leads to substantially smaller reductions for both the air and the helium injection. At the largest flow rates, the helium data indicate skin friction ratios near one. Photographs taken under these conditions show that the bubbles have in fact left the boundary layer region. The helium results have apparently returned to their undisturbed drag value, within the scatter, because buoyancy effects (stronger at higher gas flow rates because of the larger bubble sizes [15]) have made the bubbles ineffective as drag reducers. The effect of buoyancy on the denser air is not as strong.

Drag reduction data taken at a mean speed of 7.6 m/sec are shown in Fig. 5. Here the initial drag overshoot is absent, suggesting that the undisturbed boundary layer is fully developed at this speed. The drag reduction for both the helium and air is roughly the same, in agreement with the work of MDM [1]. Note, however, that the maximum drag reduction at this speed is larger than at 4.6 m/sec. This would seem to indicate that strong buoyant effects are absent at and above speeds of 7.6 m/sec.

The drag reduction data for free stream speeds of both 10.7 and 16.8 m/sec are quite similar. At both speeds, the drag reductions seems to be (slowly) leveling off at high gas flow rates. Hughes et al. [15] predicted that initial bubble size would grow proportional to $\sqrt{Q}$. Bubble sizes would likely remain larger at high gas flow rates as the small scale turbulence, most effective at breaking them down, would be destroyed by the drag reduction mechanism. One might speculate then that the larger bubbles produced at the higher gas flow rates (perhaps because they are influenced more by buoyancy) are less effective at reducing drag. The data taken at 10.7 m/sec show large reductions in skin friction for both air and helium injection; the maximum drag reduction for air injection occurs at this tunnel speed. Larger air flow rates than were available would be needed to see if

the reduction with air injection has the same high gas flow rate asymptote as the helium injection at a free stream speed of 10.7 m/sec. At a tunnel speed of 16.8 m/sec, helium injection is clearly a more effective skin friction reducer than is air injection. At an air flow rate of 4.0×10^{-3} m^3/sec, for example, a skin friction drag reduction of about 60% is obtained with helium as opposed to 40% for air. This result, although intriguing, is not well understood. Note that neither the simple computational work of MDM [9], nor the analytical work of Legner [10] provides any mechanism for describing these differences. Clearly more analytical work is needed.

Conclusion

The injection of gas to form microbubbles in a liquid turbulent boundary layer has been shown, through a series of water tunnel tests to be effective in reducing skin friction drag on an axisymmetric body. Both helium and air were used in the experiments.

Injection of helium (at high speeds) and air (at moderate speeds) produced large skin friction reductions of roughly 80 and 55% respectively. The observation that the amount of drag reduction was a function of gas type (density) was unexpected since earlier observations by MDM [1] suggested that the drag reductions obtained were essentially dependent on the volumetric, not the mass flow rate of the gas. Additional studies in the simpler flat plate geometry appear to be warranted.

The skin friction reduction increased monotonically with the gas flow rate at all but the lowest tunnel velocity tested. At this lowest speed, of 4.6 m/sec, the drag data show both an initial increase with gas injection and an optimal gas flow rate above which the drag value begin to rise. The initial drag rise is probably due to the bubble induced change in the transitional boundary layer at 4.6 m/sec.

Based on simple extrapolation of the flat plate studies [1-7], the observation of larger drag reduction at the higher tunnel speeds is an unexpected result. The differing results are apparently due to the differing influence of buoyancy in each geometry. It appears that higher free stream velocities are needed in the axisymmetric geometry to sustain effective concentrations of bubbles in the boundary layer. Certainly from a practical standpoint, the observation that maximum drag reduction, while equivalent to the flat plate value, is found at 17 m/sec rather than at 5 m/sec is a major result. The fact that the same maximum drag reduction was obtained in each experiment at (nearly the same) high gas flow rates is also of importance as the MDM boundary layer had outer scales as much as twice that of the current work while the inner scales were nearly the same. This would seem to imply, as did the simple computational studies [9], that scale up calculations, for example, should be based on inner not outer scaling. (This, of course, presupposes that the bubble concentration profiles can be made to peak in the near wall region and persist there, independent of the geometry of the boundary layer.)

It is apparent from all the experiments done to date that large reductions in skin friction [1-7] and total drag [8] may be obtained by using gas injection in a liquid turbulent boundary layer, provided that a sufficient concentration of (sufficiently small) bubbles can be maintained in the near wall region. The extrapolation of these results to practical geometries at practical Reynolds number, as well as calculations of the gas flow rate necessary, is very much dependent on the dynamics of the bubbles in these situations. Information on bubble trajectories and bubble sizes (and the evolution of sizes in the changing turbulent field) are necessary. The theoretical framework to formulate such a view of bubble dynamics is currently lacking. Experiments, in which the influence of various parameters (e.g., pressure gradient, density) on the drag reduction is catalogued, or in which the phenomenon is examined in boundary layers with widely different inner or outer flow parameters, should be useful in providing insight for theoretical models.

Acknowledgment

This work was supported by the Naval Sea Systems Command under Contract N00024-79-6-60403. Professor George B. Gurney designed the force balance. Discussions between the authors and Professor Charles L. Merkle of the Mechanical Engineering Department at Penn State were very helpful.

Table 1. Comparison of LDA Data

Variables	MDM Flat Plate	Axisymmetric
Downstream Location (mm)	454*	413**
U_∞ (m/s)	10.47	11.25
R_θ (1.607)	10,627	6,611
H	1.25	1.27
U_* (m/s)	0.3898	0.449
C_f	0.0028	0.0032
Location (mm)	374	285
U_∞ (m/s)	10.30	11.15
R_θ (1.883)	8,862	4,707
H	1.28	1.27
U_* (m/s)	0.3962	0.466
C_f	0.0029	0.0035
Location (mm)	272	155
U_∞ (m/s)	10.90	11.09
R_θ (2.271)	7,358	3,240
H	1.27	1.29
U_* (m/s)	0.4222	0.477
C_f	0.0030	0.0037

*From virtual origin

**From trip wire

List of References

1. Madavan, N. K., S. Deutsch and C. L. Merkle. Physics of Fluids 27:356 (1984a).

2. Madavan, N. K., S. Deutsch and C. L. Merkle. Journal of Fluid Mechanics 156:237 (1985).

3. Madavan, N. K., S. Deutsch and C. L. Merkle. AIAA Paper 84-0348 (1984b).

4. Migirenko, G. S. and A. R. Evseev. Problems of Thermophysics and Physical Hydrodynamics (in Russian), (Novosibirsk), Nauka (1974).

5. Dubnishchev, Yu. N., E. R. Evseev, V. S. Sobolev and E. N. Utkin. Journal of Applied Mechanics and Technical Physics 16(1):114 (1975).

6. Bogdevich, V. G. and A. G. Maliuga. Investigations of Boundary Layer Control (in Russian), edited by S. S. Kutateladze and G. S. Migirenko (Thermophysics Institute Publishing House), p. 62 (1976).

7. Bugdevich, V. G. and A. R. Evseev. Investigations of Boundary Layer Control (in Russian), edited by S. S. Kutateladze and G. S. Migirenko (Thermophysics Institute Publishing House), p. 49 (1976).

8. McCormick, M. E. and R. Bhattacharyya. Naval Engineers Journal 85:11 (1973).

9. Madavan, N. K., S. Deutsch and C. L. Merkle. Proceedings of the 1984 Symposium on Laminar Boundary Layers, ASME Fluids Engineering Conference, New Orleans, LA (1984) -- to appear in Journal of Fluids Engineering.

10. Legener, H. H. Physics of Fluids 27:2788 (1984).

11. Lumley, J. L. Physics of Fluids 20(10):S65-S71, Part II (1977).

12. Merkle, C. L. and S. Deutsch. AIAA Paper 85-0537 (1985).

13. Fortuna, G. and T. J. Hanratty. Journal of Fluid Mechanics 53:575, Part III (1972).

14. Zierke, W. C. and S. Deutsch. ARL/PSU Technical Memorandum 85-85, Applied Research Laboratory, The Pennsylvania State University (1985).

15. Hughes, N. H., M. M. Reischman and J. M. Holzman. Sixth Biennial Symposium on Turbulence, The University of Missouri, Rolla, MO (1979).

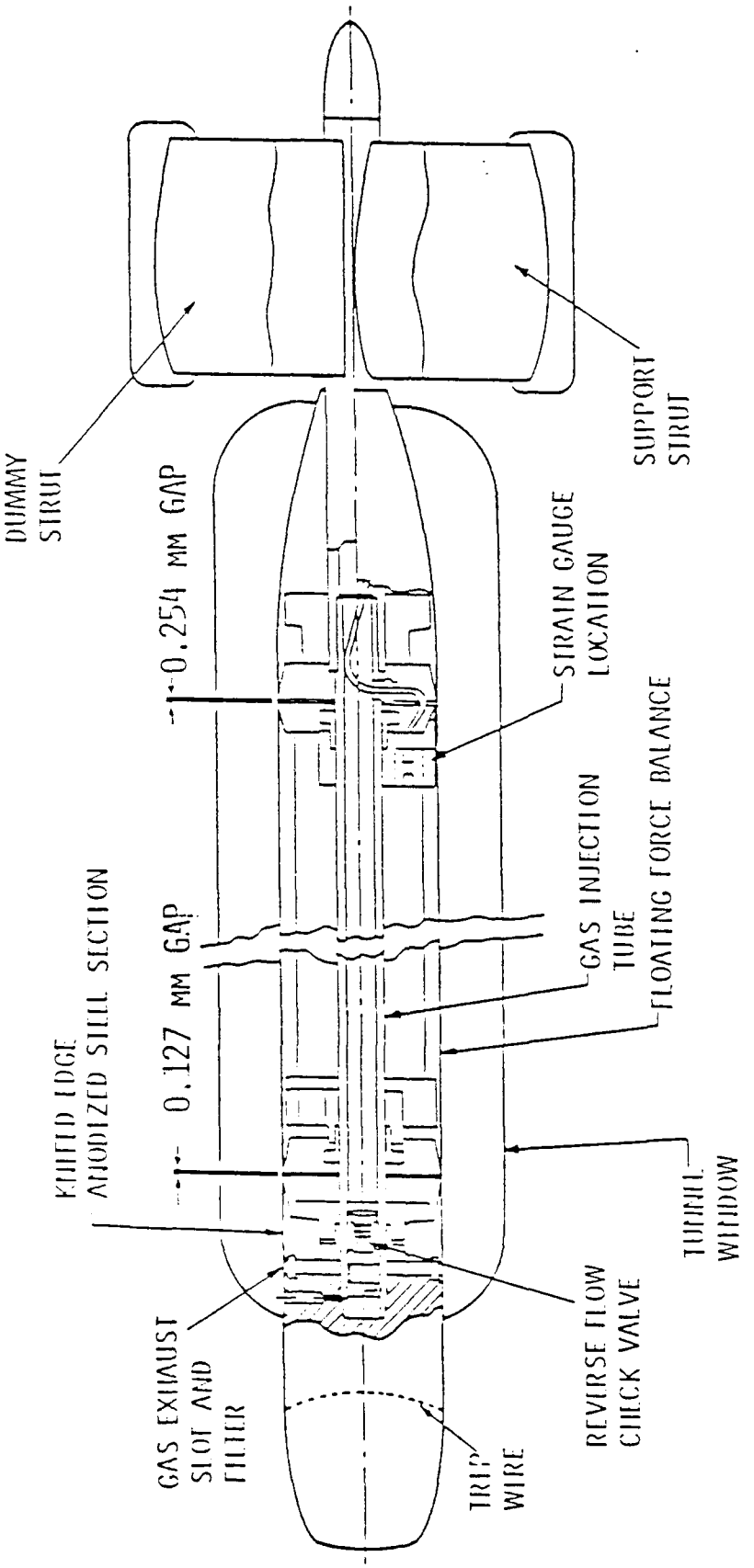

Figure 1. Axisymmetric Skin Friction Model.

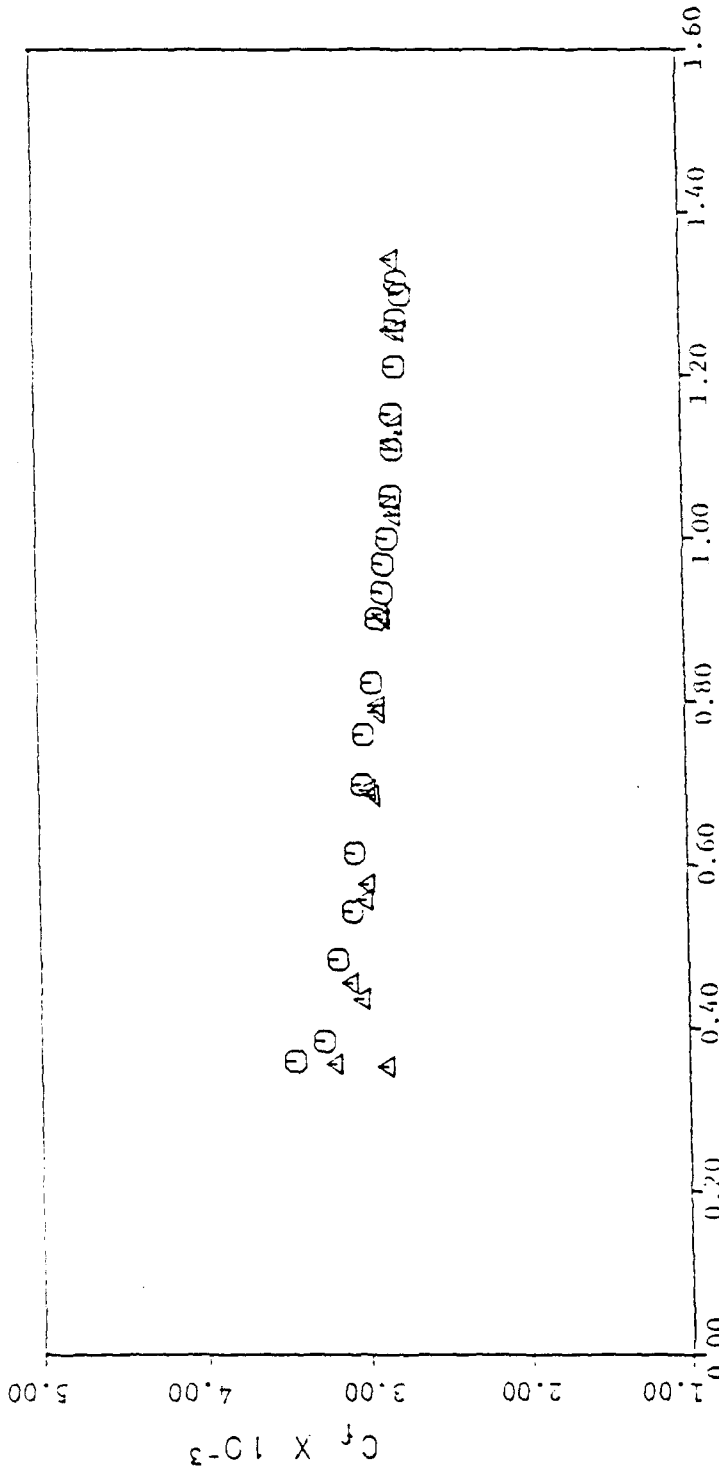

Figure 2. Skin Friction Drag Coefficient versus Maximum Diameter Reynolds Number.

2 August 1985
SD:JC:lhz

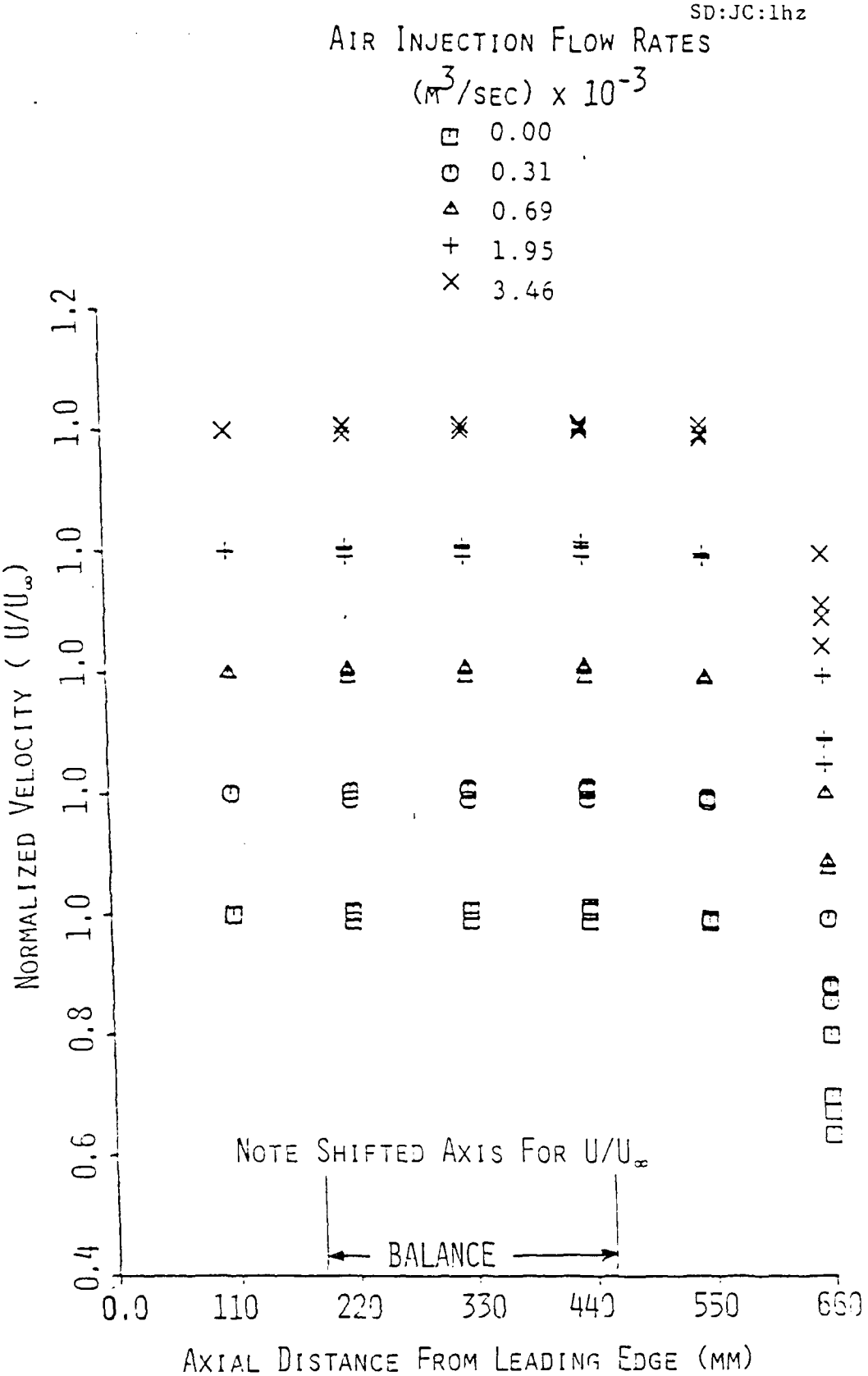

Figure 3. Normalized Velocity Distribution Determined from Static Pressure Measurements.

2 August 1985
SD:JC:lhz

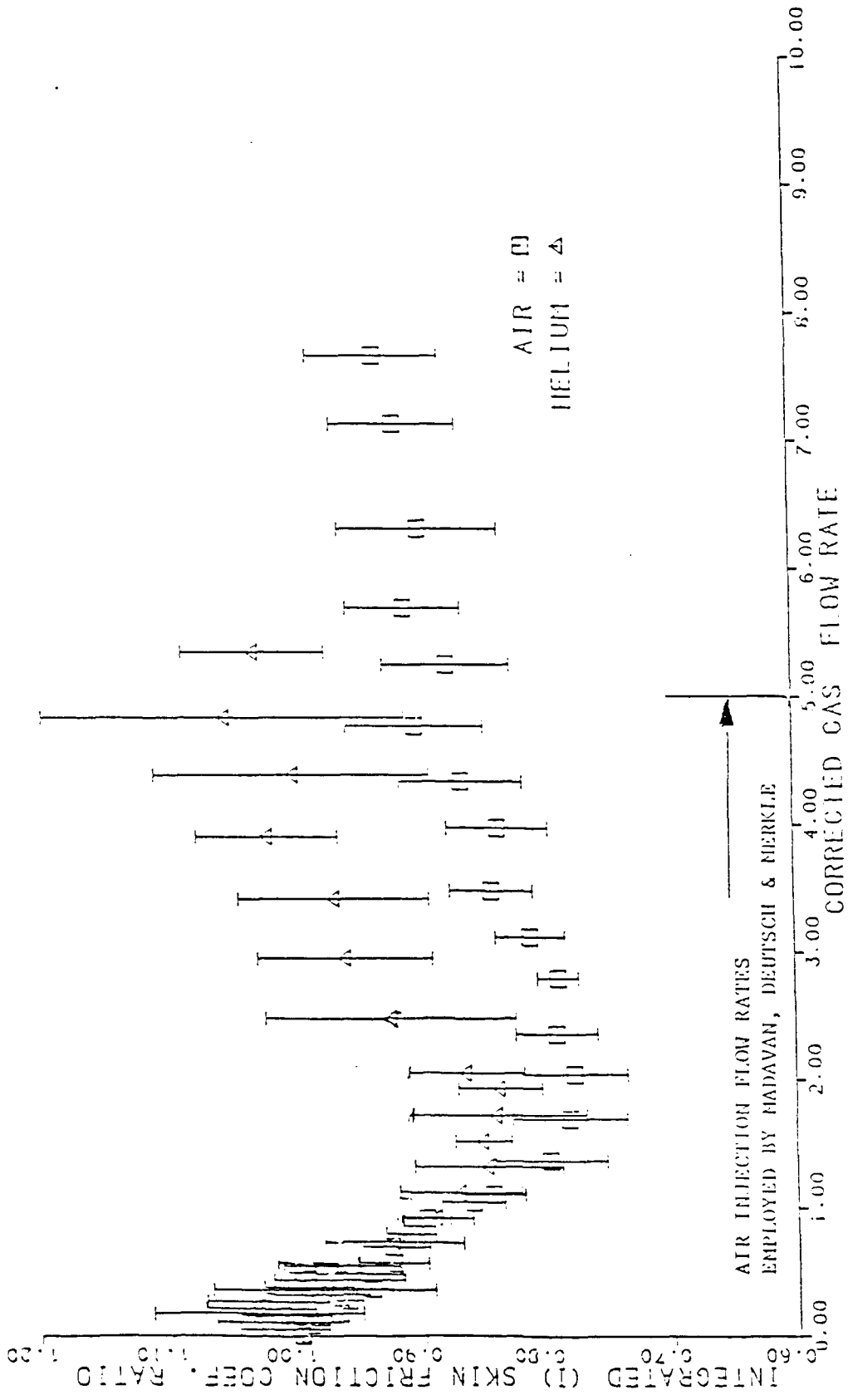

Figure 4. Drag Reduction at 4.6 m/sec.

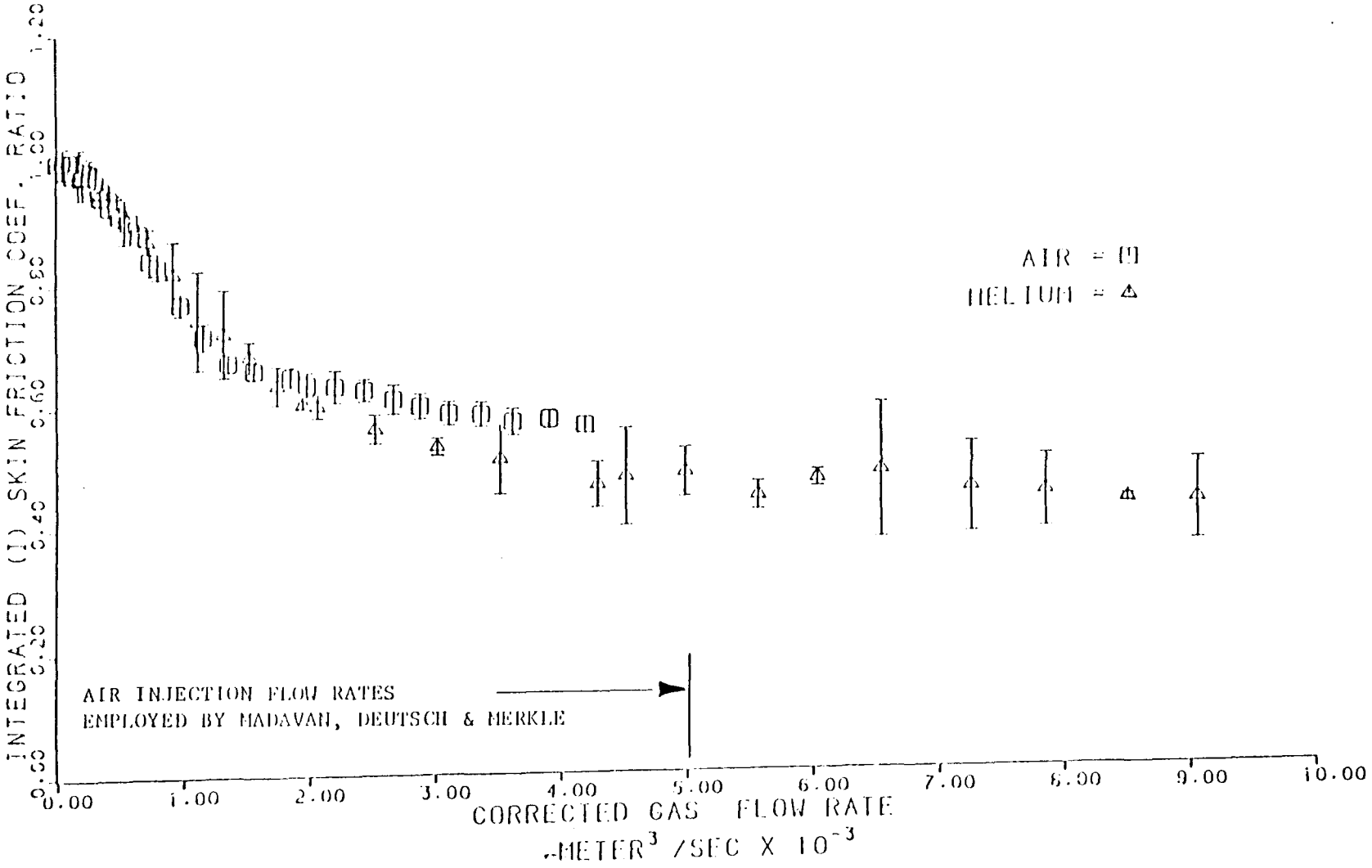

Figure 5. Drag Reduction at 7.6 m/sec.

2 August 1985
SD:JC:lhz

2 August 1985
SD:JC:lhz

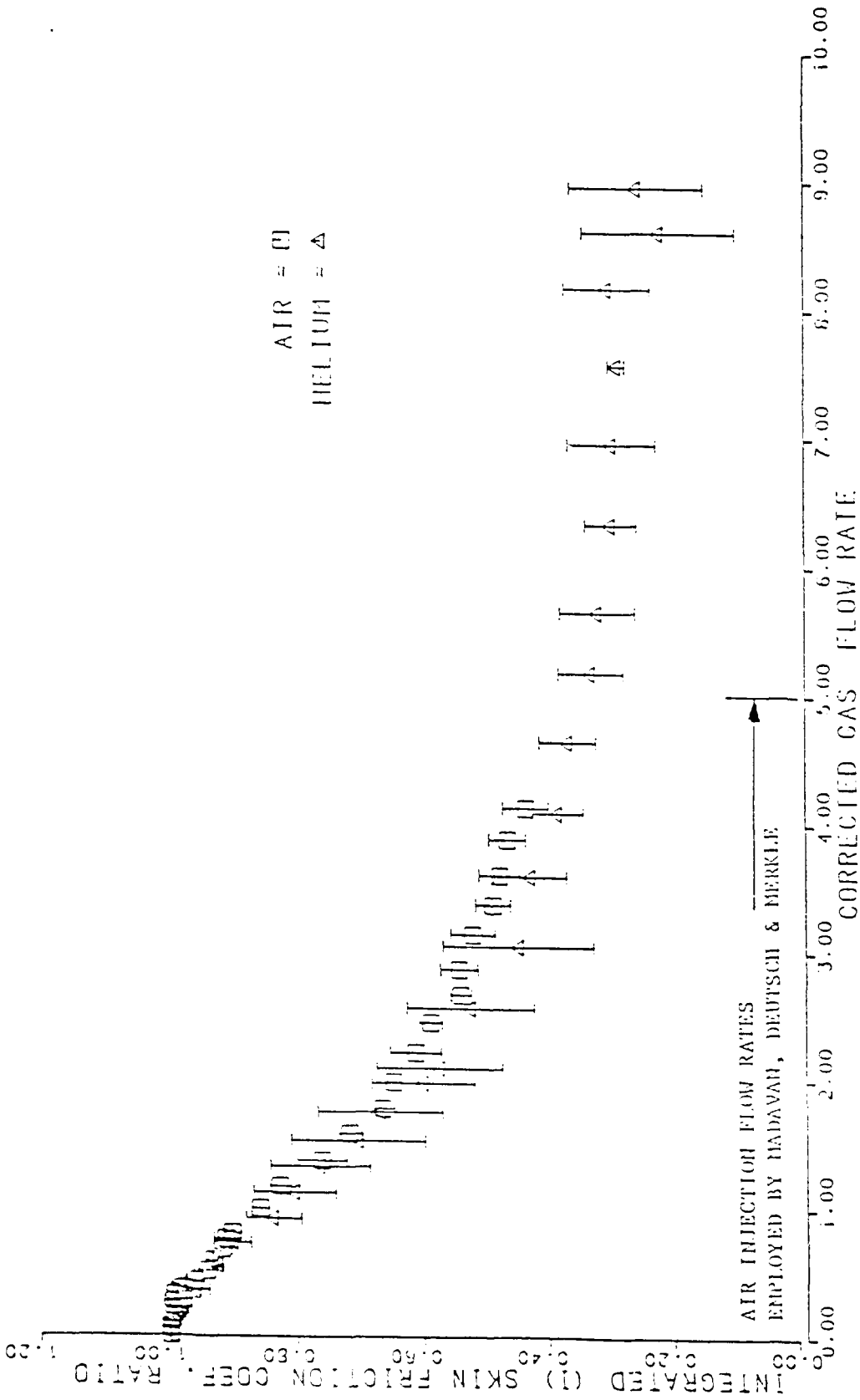

Figure 6. Drag Reduction at 10.7 m/sec.

2 August 1985
SD:JC:lhz

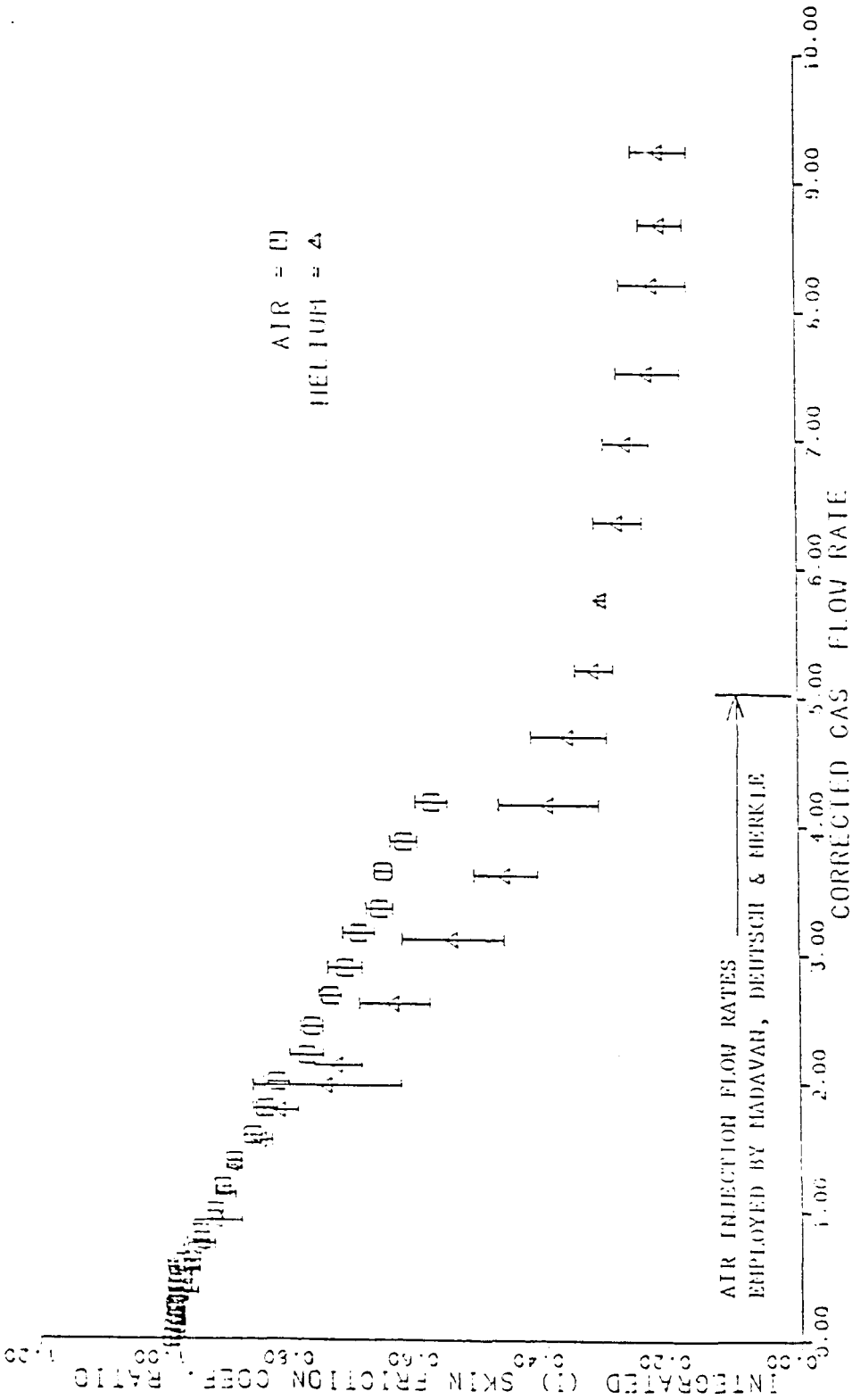

Figure 7. Drag Reduction at 16.8 m/sec.

Distribution List for ARL/PSU Unclassified TM 85-139 by S. Deutsch and J. Castano, dated 2 August 1985

Commander
Naval Sea Systems Command
Department of the Navy
Washington, DC 20362
Attn: Library
Code NSEA-09G32
(Copies 1 and 2)

Commander
Naval Sea Systems Command
Department of the Navy
Washington, DC 20362
Attn: W. D. Marlin
Code NSEA-913TM3
(Copy No. 3)

Commander
Naval Sea Systems Command
Department of the Navy
Washington, DC 20362
Attn: A. R. Paladino
Code NSEA-55N
(Copy No. 4)

Commander
Naval Sea Systems Command
Department of the Navy
Washington, DC 20362
Attn: T. E. Peirce
Code NSEA 63R-31
(Copy No. 5)

Commander
Naval Sea Systems Command
Department of the Navy
Washington, DC 20362
Attn: F. J. Romano
Code NSEA-63R
(Copy No. 6)

Commanding Officer
Naval Underwater Systems Ctr.
Department of the Navy
Newport, RI 02840
Attn: Library
Code 54
(Copy No. 7)

Commanding Officer
Naval Underwater Systems Ctr.
Department of the Navy
Newport, RI 02840
Attn: T. A. Davis
Code 36301
(Copy No. 8)

Commanding Officer
Naval Underwater Systems Ctr.
Department of the Navy
Newport, RI 02840
Attn: D. J. Goodrich
Code 3639
(Copy No. 9)

Commanding Officer
Naval Underwater Systems Ctr.
Department of the Navy
Newport, RI 02840
Attn: C. L. Hervey
Code 3634
(Copy No. 10)

Commanding Officer
Naval Underwater Systems Ctr.
Department of the Navy
Newport, RI 02840
Attn: R. H. Nadolink
Code 3634
(Copy No. 11)

Commanding Officer
Naval Underwater Systems Ctr.
Department of the Navy
Newport, RI 02840
Attn: C. N. Pryor
Code 01
(Copy No. 12)

Officer-in-Charge
David W. Taylor Naval Ship
Research & Development Ctr.
Department of the Navy
Bethesda, MD 20084
Attn: T. T. Huang
Code 1542
(Copy No. 13)

Distribution List for ARL/PSU Unclassified TM 85-139 by S. Deutsch and J. Castano, dated 2 August 1985 [continuation]

Officer-in-Charge
David W. Taylor Naval Ship
Research & Development Ctr.
Department of the Navy
Bethesda, MD 20084
Attn: J. H. McCarthy
Code 154
(Copy No. 14)

Officer-in-Charge
David W. Taylor Naval Ship
Research & Development Ctr.
Department of the Navy
Bethesda, MD 20084
Attn: J. J. Shen
Code 1940
(Copy No. 15)

Officer-in-Charge
David W. Taylor Naval Ship
Research & Development Ctr.
Department of the Navy
Bethesda, MD 20084
Attn: M. M. Sevik
Code 19
(Copy No. 16)

Commander
Naval Surface Weapons Center
Detachment
White Oak Laboratory
10901 New Hampshire Avenue
Silver Spring, MD 20903-5000
Attn: G. C. Guanaurd
(Copy No. 17)

Office of Naval Research
800 North Quincy Street
Department of the Navy
Arlington, VA 22217
Attn: M. M. Reischman
Code 432F
(Copy No. 18)

Office of Naval Research
800 North Quincy Street
Department of the Navy
Arlington, VA 22217
Attn: R. E. Whitehead
Code 432
(Copy No. 19)

Naval Research Laboratory
Department of the Navy
Washington, DC 20390
Attn: R. J. Hansen
(Copy No. 20)

Naval Research Laboratory
Department of the Navy
Washington, DC 20390
Attn: E. W. Hendricks
(Copy No. 21)

Rand Corporation
1700 Main Street
Santa Monica, CA 90406
Attn: J. Aroesty
(Copy No. 22)

Rand Corporation
1700 Main Street
Santa Monica, CA 90406
Attn: C. Gazley
(Copy No. 23)

Rand Corporation
1700 Main Street
Santa Monica, CA 90406
Attn: R. King
(Copy No. 24)

Rand Corporation
1700 Main Street
Santa Monica, CA 90406
Attn: A. R. Wazzan
(Copy No. 25)

Distribution List for ARL/PSU Unclassified TM 85-139 by S. Deutsch and J. Castano, dated 2 August 1985 [continuation]

Dynamics Technology, Inc.
22939 Hawthorne Blvd.
Torrance, CA 90505
Attn: G. L. Donohue
(Copy No. 26)

Dynamics Technology, Inc.
22939 Hawthorne Blvd.
Torrance, CA 90505
Attn: W. W. Haigh
(Copy No. 27)

Professor T. J. Hanratty
Department of Chemical Engineering
205 Roger Adams Lab C-3
The University of Illinois
Urbana, IL 61801
(Copy No. 28)

Mr. P. S. Klebanoff
National Bureau of Standards
771.FM105
Washington, DC 20234
(Copy No. 29)

Dr. J. L. Lumley
Sibley School of Engineering
Cornell University
Ithaca, NY 14850
(Copy No. 30)

Dr. N. K. Madavan
Ingersol-Rand Research Inc.
Post Office Box 301
Princeton, NJ 08542
(Copy No. 31)

Mr. J. M. McMichael
AFOSRINA
Building NO. 410
Bolling AFB-DC 20332
(Copy No. 32)

Dr. R. F. Mons
Westinghouse Electric Corp.
Post Office Box 1458
Annapolis, MD 21404
(Copy No. 33)

Dr. W. M. Phillips
Department of Mechanical Engineering
Purdue University
Lafayette, IN 47907
(Copy No. 34)

Professor W. G. Tiederman
Department of Mechanical Engineering
Purdue University
Lafayette, IN 47907
(Copy No. 35)

Applied Research Laboratory
The Pennsylvania State University
Post Office Box 30
State College, PA 16804
Attn: J. Castano
(Copy No. 36)

Applied Research Laboratory
The Pennsylvania State University
Post Office Box 30
State College, PA 16804
Attn: S. Deutsch
(Copy No. 37)

Applied Research Laboratory
The Pennsylvania State University
Post Office Box 30
State College, PA 16804
Attn: G. B. Gurney
(Copy No. 38)

Applied Research Laboratory
The Pennsylvania State University
Post Office Box 30
State College, PA 16804
Attn: R. E. Henderson
(Copy No. 39)

Applied Research Laboratory
The Pennsylvania State University
Post Office Box 30
State College, PA 16804
Attn: L. R. Hettche
(Copy No. 40)

Applied Research Laboratory
The Pennsylvania State University
Post Office Box 30
State College, PA 16804
Attn: G. C. Lauchle
(Copy No. 41)

Applied Research Laboratory
The Pennsylvania State University
Post Office Box 30
State College, PA 16804
Attn: C. L. Merkle
(Copy No. 42)

Applied Research Laboratory
The Pennsylvania State University
Post Office Box 30
State College, PA 16804
Attn: B. R. Parkin
(Copy No. 43)

Applied Research Laboratory
The Pennsylvania State University
Post Office Box 30
State College, PA 16804
Attn: GTWT Files
(Copy No. 44)

Applied Research Laboratory
The Pennsylvania State University
Post Office Box 30
State College, PA 16804
Attn: ARL/PSU Library
(Copy No. 45)